CHAPTER (V)

EFFECT OF FLUID SATURATION ON ACOUSTIC WAVE VELOCITY

CHAPTER 5
EFFECT OF FLUID SATURATION ON ACOUSTIC WAVE VELOCITY

Seismic body waves exist in two types, as compressional wave and shear wave with the velocities V_p and V_s. The velocity of propagation in an isotropic elastic medium is a function of Lame's parameters and rock density. These parameters may be expressed in terms of bulk modulus, shear modulus and Poisson's ratio. In the present work, compressional and shear velocities were measured at room temperature and ambient pressure on cylindrical samples using a two channels Sonic Viewer (OYO - 170) in the petrophysical lab of the Department of Geophysics at Ain Shams University, Cairo. The instrument performs fast sampling and digital recording. Stacking in 16 bit memory improves the signal to noise ratio and widens its applicability to weak signals. The p-wave and s-wave velocities have been measured at ultrasonic frequencies of 63 kHz and 33 kHz, respectively.

The use of seismic waves for determining reservoir rock properties is of great value to hydrocarbon zonation and exploration. The acoustic properties of rocks control the relations between an alternating stress of various frequencies and corresponding strains. Seismic waves velocities for gas, water and oil reservoirs are early discussed by many investigators **(e.g. Wyllie et al., 1958, Nur and Simmon, 1969, Elliot and Wiley, 1975, Gregory, 1976, El Sayed et al., 1998 & 1999,** and **Salah, 2001).** The effect of both fluid saturation and stresses on dynamic elastic properties of some clastic and carbonate reservoir rocks was studied by many investigators **(e.g. Biot, 1956a, b, Gregory, 1976,** and **El Sayed et al., 1997).**

Compressional and shear waves have different behavior in rocks depending on difference in porosity, fluid saturation, fluid viscosity, density, laminations, fracturing, clay content, mineralogy, compaction and pore space framework. The velocity ratio of compressional and shear waves (V_p/V_s) varies in crystalline and metamorphic rocks within a very narrow range (from 1.7 to 1.9). In sedimentary rocks, it varies in a wider range from 1.5 to 14.0 due to the very low shear strength of highly porous rocks ($\Phi > 25\%$).

Biot (1956b) investigated the seismic wave propagation at high frequencies in an isotropic, liquid–saturated porous medium. Two main conclusions may be drawn from Biot's analysis. First, the shear wave velocity values in a liquid–saturated porous material will always be less than that in the dry material based on an assumption that micro-cracks are

negligible. Second, the compressional wave velocity values in the liquid–saturated porous material will generally be higher than that in the dry case, except for material having low bulk compressibility. The technique used to measure acoustic wave velocity is the pulse first arrival technique, in which the travel time is determined for a pulse of compressional or shear waves to pass a known measured thickness of the rock (sample length).

P-wave and s-wave velocities values (at different saturation) have been determined on a subset of 26 samples. The p-wave and s-wave velocities were measured with the sample fully saturated with air (dry, $Sw = 0$) and partially saturated with brine water ($Sw = 25\%$, 50% and 75%) and fully saturated with brine water ($Sw = 100\%$). The samples were saturated with brine using imbibition technique. This technique allowed samples to be saturated with brine according to its capillary configuration. The measured values of compressional V_p and shear wave velocity V_s at different saturation levels for the 26 investigated samples are listed in Tables (5-1) and (5-5) respectively of appendix 4.

5-1. Compressional and shear wave velocity at different saturation levels

The cleaned samples were dried at a drying oven (105^0C) for 12 hours as an initial period of drying. The samples were removed after constant weights were achieved. Samples were considered to have constant weight when the weight taken before and after a subsequent 4 hours drying period is repeatable to less than $\pm$ 2%. In the studied samples, the compressional wave velocity V_p of dry samples varies from 2310 m/s to 4000 m/s with a mean value of 2996 m/s. The shear wave velocity V_s of dry samples varies from 1390 m/s to 2690 m/s with a mean value of 2051 m/s.

25% brine and 75% gas

The imbibitions technique was chosen to saturate the samples at that system. The imbibitions technique has many advantages over the flow one **(Domenico, 1976).** The imbibition technique allows the sample to imbibe the brine according to its capillary configuration. The samples covered by brine were put in a dessicator designed in a way to apply vacuum (-200 kPa) inside it. The vacuum was applied for a course of seconds, weights of partially saturated samples were checked (unleached paper was used to remove the excess brine from the sample surface). If the samples saturation was close to the desired saturation, the samples were put under brine and left for minutes (without vacuum). Again the sample weight was checked. The procedure was repeated until the desired

weight was achieved. Once the saturation levels had been achieved, the samples were preserved in saran wrap and aluminum foil and kept at constant room temperature for 24 hours. That course of time was given to allow the fluid redistribution inside the samples according to its capillary and pore spaces configuration. It was difficult to adjust the saturation level at exactly the predetermined level, $\pm$ 2% saturation percent was considered to be the accepted limit of the predetermined level. Evaporation of fluids was not used to adjust the saturation level. The evaporation might increase the salinity of the remaining fluid inside the samples or salt crystals might have precipitated inside the pore spaces. In the studied samples, the compressional wave velocity V_p of saturated samples at 25% varies from 1820 m/s to 4100 m/s with a mean value of 3006 m/s. Shear wave velocity V_s of saturated samples at 25% varies from 1120 m/s to 2270 m/s with a mean value of 1711 m/s.

50% brine – 50% gas system

The saturation levels of that system were achieved by the same procedure that was described in the previous system. In the studied samples, the compressional wave velocity V_p of saturated samples at 50% varies from 1870 m/s to 4320 m/s with a mean value of 3250 m/s. Shear wave velocity V_s of saturated samples at 50% varies from 1040 m/s to 1910 m/s with a mean value of 1448 m/s.

75% brine – 25% gas system

The predetermined saturation level of 75% brine was achieved by imbibition technique. In the studied samples, the compressional wave velocity V_p of saturated samples at 75% varies from 2220 m/s to 4430 m/s with a mean value of 3320 m/s. Shear wave velocity V_s of saturated samples at 75% varies from 1070 m/s to 1860 m/s with a mean value of 1446 m/s.

100% brine system

The partially saturated samples were put under brine and until no air bubbles had been coming out of the samples. The samples were then loaded in a pressure saturator and the pressure was raised up to 13790 kPa. and the system was kept pressurized for two hours. This process will force the trapped air in the small pore spaces to be dissolved in the brine. Again, the samples were put under brine and vacuum. This step is necessary to drive out the dissolved air of the previous step. The steps were repeated until at least 98% saturation was achieved. The decrease in saturation is believed to be due to grain loss and rough grain surfaces in

some samples. For the fully saturated samples, the compressional wave velocity V_p varies from 2930 m/s to 4560 m/s with a mean value of 3635 m/s. The shear wave velocity V_s of the fully saturated samples varies from 1110 m/s to 2160 m/s with a mean value of 1538 m/s.

The relationships between compressional and shear wave velocity are shown in Fig. 5-1 for full (Sw = 100%) or partial saturation with brine. This relation reveals that the compressional wave velocity V_p increases in consistence with the increase of shear wave velocity V_s at all levels of partial fluid saturation. The slope of the regression line shows a gradual decrease with increasing brine saturation. It can be observed that shear wave velocity decreases gradually with brine saturation and reaches the lowest value at Sw = 75%. A further increase in saturation towards Sw = 100% results in a slight increase of velocity.

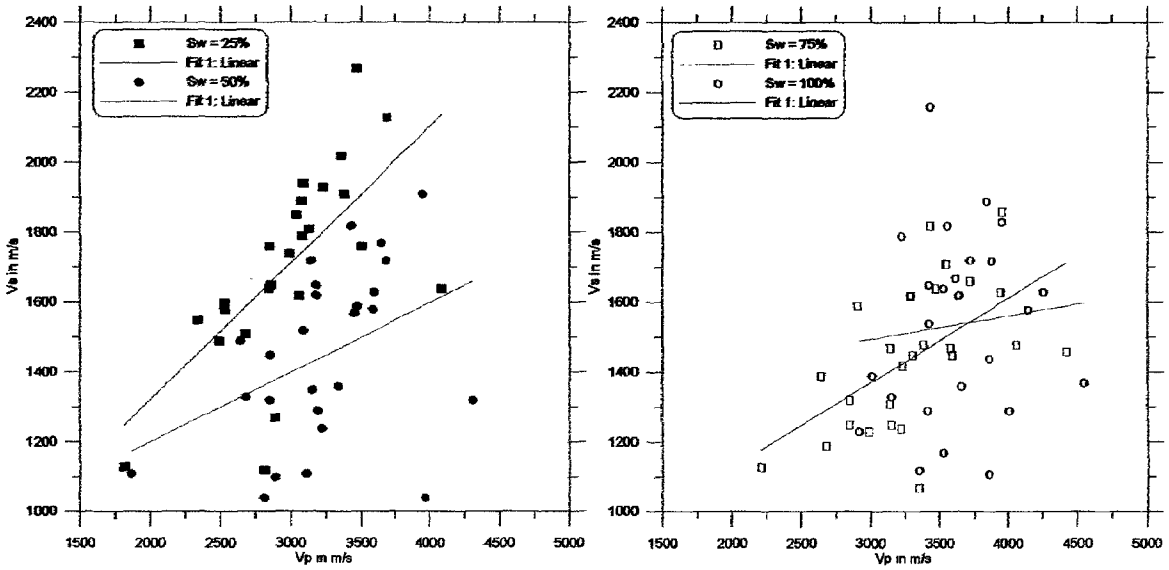

Fig. 5-1 Compressional V_p versus shear wave velocity V_s at different saturation levels. 26 data points are used.

5-2. Effect of brine saturation on compressional wave velocity

The effect of brine saturation at different levels is shown in Fig. 5-2. In the dry state (100% gas saturation), the average of the compressional wave velocity was found to be 2996 m/s. When the saturation was increased at 25%, a velocity increase was observed for most samples. Only for a small number of samples, the velocity remains at the same level. The calculated average velocity at 25% saturation was equal to 3006 m/s. When the brine saturation was increased to be 50% and 75%, the average velocities were increased to 3250 and 3320 m/s, respectively. At the brine saturation of 100%, all the velocities were increased. The average compressional wave velocity was found to be 3635 m/s. In general, the average compressional wave velocity increases gradually

with increasing saturation. The highest recorded velocities of all the samples were determined at full saturation with brine.

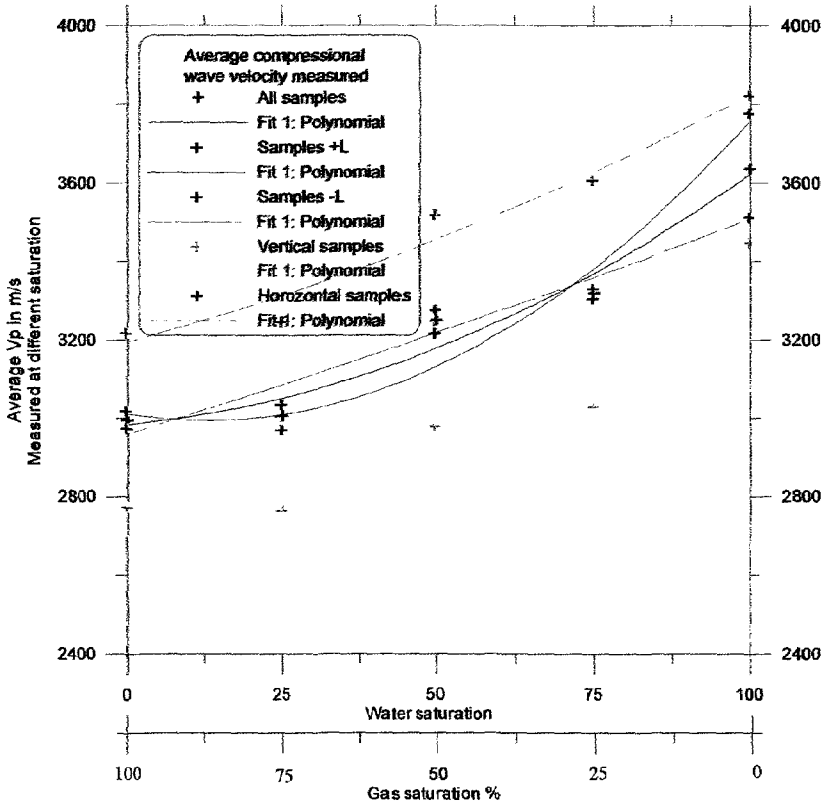

Fig. 5-2 Average of compressional wave velocity versus gas - brine saturation.

5-3. Effect of saturation on shear wave velocity

The effect of brine saturation on shear wave velocity is shown in Fig. 5-3. For the dry state, the average value of the shear wave velocity was found to be 2051 m/s. When the brine saturation was increased to be 25%, 50% and 75%, the average of shear wave velocity decreased to be 1711, 1448 and 1446 m/s respectively. At 100% brine saturation, the average velocity increased to a value of 1538 m/s. The highest recorded velocities of all the samples were determined at dry state or full saturation with air.

Numerous theoretical models have been proposed to describe elastic wave propagation in two-phase sedimentary rocks of finite porosity. Perhaps the most successful of these is the model of **Biot (1962).** The Biot model requires knowledge on the elastic properties of the matrix material, pore fluid saturation, and the elastic properties of the frame or skeleton composing the matrix. The elastic properties of the frame are determined empirically, with little theoretical consideration given to the pore geometry creating the non – uniform porosity. **Geertsma and Smith**

(1961) have noted an anomalous behavior of shear wave velocities in certain liquid saturated sandstones.

King (1966) has shown that at lower confining pressures the shear wave velocity for kerosene saturated sandstone is higher than for the dry rocks. It is concluded that this increase in velocity can only be explained by relaxation behavior of the liquid saturate in the small fissures or micro-cracks, which close progressively as the confining pressure is increased.

Gregory (1976) stated that the experimental data support Biot's theory for all porosities at confining pressures above 62000 kPa. However, as pressure declines, the data for low porosity rocks begin to depart from the theory. The interpretation of velocity behavior is slightly difficult due to the effect of many parameters such as rock compressibility, density of matrix and pore fluids, rigidity and rock porosity.

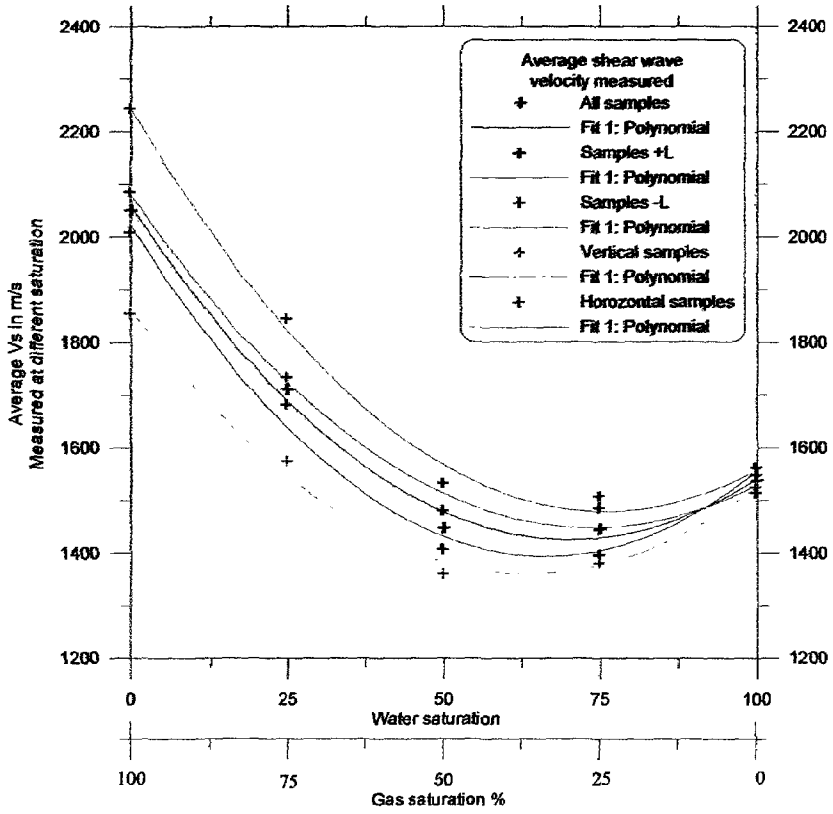

Fig. 5-3 Average of shear wave velocity versus gas - brine saturation.

5-4. Effect of saturation on Poisson's ratio

Poisson's ratio is defined as the ratio of relative lateral strain to longitudinal strain of uniaxial stress applied to a unit cube of the rock. It is computed from p-wave velocity *Vp* and s-wave velocity *Vs* by the following relation:

$$\upsilon = \frac{\left(\frac{V_P}{V_S}\right)^2 - 2}{2\left(\left(\frac{V_P}{V_S}\right)^2 - 1\right)} \qquad (1)$$

with

V_P = compressional wave velocity, and

V_S = shear wave velocity.

Poisson's ratio varies over a range $0.0 < \upsilon < 0.5$ for all types of dry and saturated rocks **(Nur and Simmon, 1969, Gregory, 1976, El-Sayed et al., 1997).** In addition, Poisson's ratio has been used as an indicator for fracture height determination in charged reservoir rocks **(Gregory, 1976).** The range of Poisson's ratio for isotropic materials is limited to less than 0.5 for theoretical reasons. Poisson's ratio varies over a wide range of possible values including negatives values **(Gregory, 1976).** Negatives Poisson's ratio is observed for real sedimentary rock.

When rigidity is zero, no shear wave can be transmitted and Poisson's ratio is 0.50. Most rocks possess sufficient rigidity to transmit shear waves. Consequently, most rocks have Poisson's ratio less than 0.50. The Poisson's ratio is of importance in some aspects of seismic exploration for gas and oil. It should be noted that Poisson's ratio decreases with depth as a consequence of linking *Vp* with *Vs* at common depths. The p-wave velocity alone may not be sufficient to identify zones of partial saturation or gas saturation. Since s-wave velocity is less sensitive to the final saturation than the p-wave, it can be used as a normalizing quantity with which to compare p-wave velocity and the ration *Vp/Vs*. The measured values of Poisson's ratio at different saturation levels for the 26 investigated samples are listed in Table 5-8 of appendix 4 and presented in Fig. 5-4.

At 100% gas saturation, the Poisson's ratio shows positive and negative values with a wide range of variation from -0.093 to 0.351 with an average of 0.042. The negative values may be caused by slight inaccuracies in the determination of p- and s-wave velocities. Since the determination of the first break or travel times of s-waves is a complicated matter, a certain inaccuracy of s-wave velocity can be expected. A slight overestimation of s-wave velocity causes a negative Poisson's ratio.

When the samples were saturated with 25% brine, all the values have increased and become positive. The Poisson's ratio ranges from 0.115 to 0.406 with an average of 0.243. By increasing the brine

saturation to 50%, all Poisson's values show a further increase with an average of 0.363. If the brine saturation was increased to 75% the values of Poisson's ratio have become much closer to each other and range from 0.289 to 0.444 with an average of 0.376. When the brine saturation reached 100% the Poisson's ratio values have reached nearly the same average 0.379.

When the brine saturation was increased to 25% and 50% the values of Poisson's ratio have increased for all samples with no exception. Again, when the brine saturation reaches 75%, the average value of Poisson's ratio increases further for all samples. These results suggest that the Poisson's ratio is increasing with brine saturation until $\simeq$ 75%. This phenomenon could be used to monitor the brine saturation in a gas reservoir. The experimental results of **Gregory (1976)** have shown that Poisson's ratio increases with brine saturation at a constant pressure of 3447 kPa. Finally, when the brine saturation approaches 100%, the Poisson's ratio reaches an asymptotic average value. This phenomenon could be used to detect the gas–water contact due to the large difference between gas-saturated Poisson's ratio and brine-saturated value. It is worth recommending to determine Poisson's ratio to construct and validate the relationship between this parameter and brine saturation in the gas-water transitional zone.

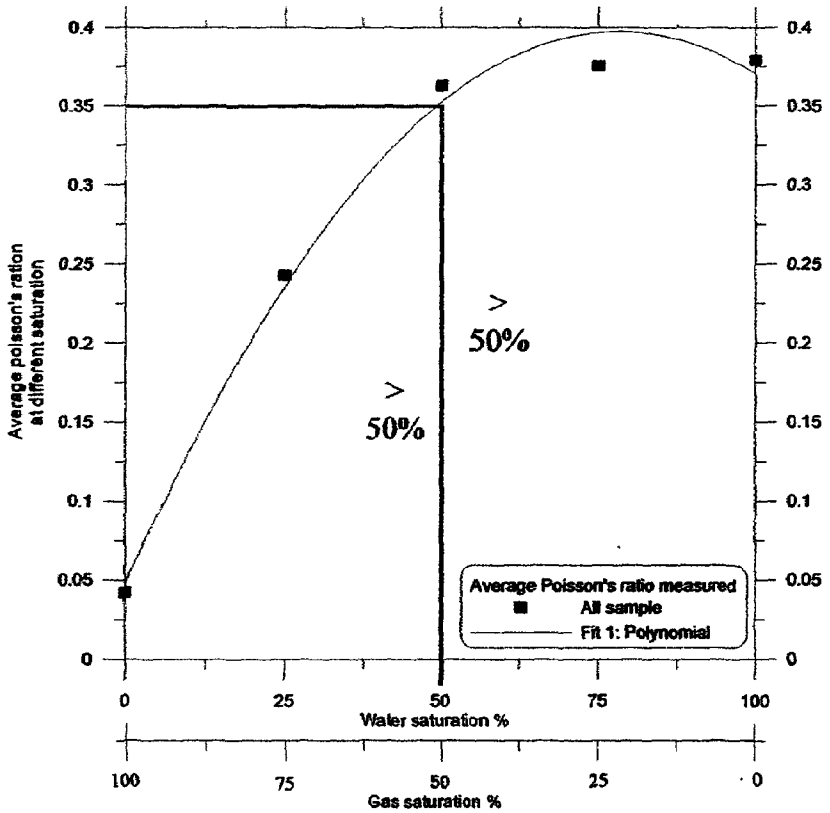

Fig. 5-4 Average of Poisson's ratio versus Gas - Brine saturation.

5-5. Theoretical approach

The discrimination between fluid and gas filling is based on a reliable prediction of the Poisson's ratio. The modeling of saturation dependent p- and s-wave velocity is the basis for the determination of a saturation dependent Poisson's ratio.

5-5.1 Compressional wave velocity and water saturation

Based on the Wyllie – equation: (see equation 17 in chapter 3)
Under dry conditions with water saturation $S_W = 0$, we get

$$\frac{1}{V_{p(dry)}} = \frac{\Phi}{V_A} + \frac{(1-\Phi)}{V_{SP}} \qquad (2)$$

with:

$V_{PS} = V_A$,

V_A = velocity in air.

Under fully saturated condition with $S_W = 1$ we get

$$\frac{1}{V_{p(sat.)}} = \frac{\Phi}{V_W} + \frac{(1-\Phi)}{V_{SP}} \qquad (3)$$

with:

V_w = velocity in water.

Considering partial saturation with $0 < S_W < 1$, the Wyllie – equation is extended

$$\frac{1}{V_p(S_W)} = \frac{\Phi S_W}{V_W} + \frac{\Phi(1-S_W)}{V_A} + \frac{(1-\Phi)}{V_{SP}}. \qquad (4)$$

or

$$\frac{1}{V_p(S_W)} = \frac{\Phi S_W}{V_W} - \frac{\Phi S_W}{V_A} + \frac{\Phi}{V_A} + \frac{1-\Phi}{V_{SP}}. \qquad (5)$$

Considering equation (2), the relation between velocity and saturation can be expressed by:

$$V_p(S_W) = \frac{1}{\Phi S_W\left(\frac{1}{V_W} - \frac{1}{V_A}\right) + \frac{1}{V_{p(dry)}}}. \qquad (6)$$

For the numerical calculation, the following values are considered:

$V_{p(dry)} \triangleq$ average velocity of dry samples,

$\Phi \triangleq$ average porosity of samples,

V_W = velocity in water (1500 m/s),

V_A = velocity in air (330 m/s).

The resulting equation can be written in the form:

$$V_p(S_W) = \frac{1}{\frac{1}{V_{p(dry)}} - 0.0023636.\Phi.S_W} \qquad (7)$$

with the limits for $S_W = 0$

$$V_p(S_W = 0) = V_{p(dry)}$$

and for $S_W = 1$,

$$V_p(S_W = 1) = \frac{1}{\frac{1}{V_{p(dry)}} - 0.0023636.\Phi}.$$

Compressional wave velocity values are extrapolated from dry samples at different saturation levels according to equation 7. Data is listed in Table 5-2 of appendix 4 and shown in Fig. 5-5. It can be observed that the extrapolated compressional wave velocities calculated at different saturation levels show higher values than the measured ones.

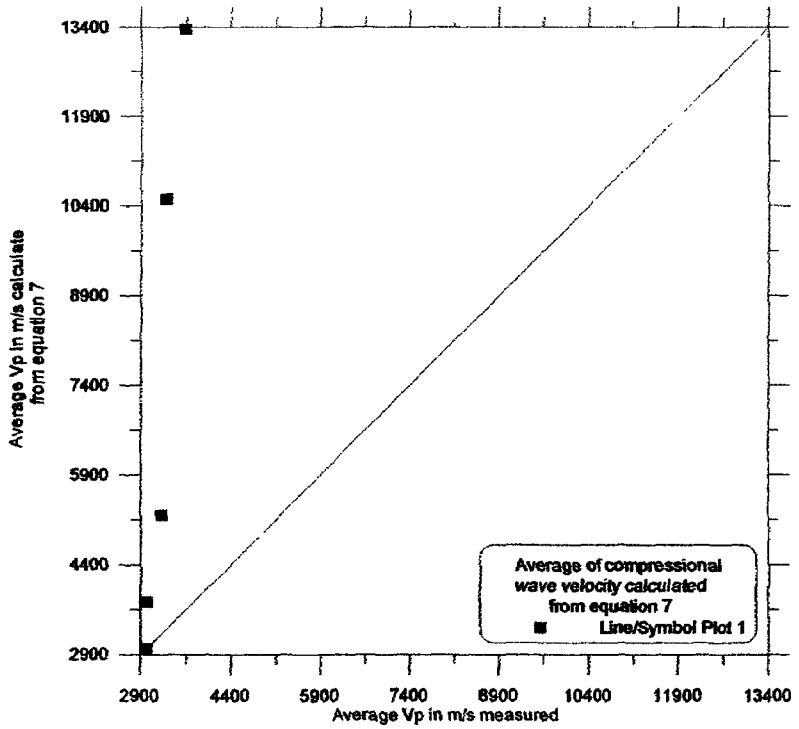

Fig. 5-5 Average of compressional wave velocity measured at different saturation levels versus average compressional wave velocity calculated from equation 7.

Starting from fully saturated samples $V_p(S_W = 1)$ (see equation 3), the saturation dependent velocity can be derived using the following equation:

$$V_p(S_W) = \frac{1}{\frac{1}{V_{p(sat.)}} + \frac{\Phi(1-S_W)}{330}}. \qquad (8)$$

with the limits for $S_W = 1$: $V_p(S_W = 1) \triangleq V_{p(sat.)}$.

Compressional wave velocity values extrapolated from the fully saturated state at different saturation levels from equation 8 are listed in Table 5-3 of appendix 4 and shown in Fig. 5-6. It can be noticed that the extrapolated compressional wave velocity calculate at different saturation levels provide lower values than the measured ones.

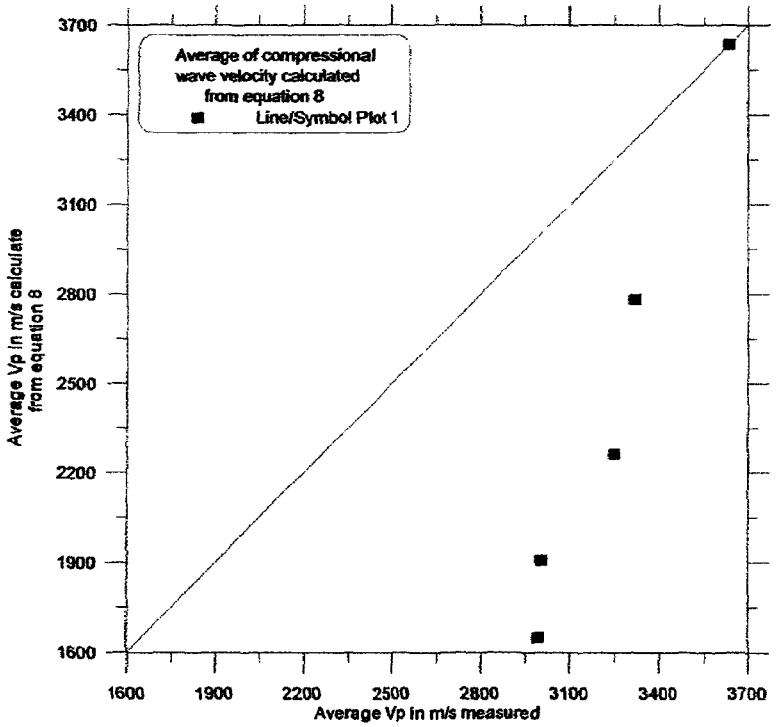

Fig. 5-6 Average of compressional wave velocity measured at different saturation levels versus average compressional wave velocity calculated from equation 8.

Equations 7 and 8 with the starting point at the dry state with $V_p(S_W = 0) = V_{p(dry)}$ and the saturated state with $V_p(S_W = 1) \triangleq V_{p(sat.)}$ are generalized with the aim that at the saturation level of 50 % the same velocity is determined:

$$V_p(S_W) = \frac{1}{\frac{1}{V_{p(dry)}} - a\Phi S_W}$$

$$V_p(S_W = 0.5) = \frac{1}{\frac{1}{V_{p(dry)}} - \frac{1}{2}a\Phi}. \quad (9a)$$

$$V_p(S_W) = \frac{1}{\frac{1}{V_{p(sat.)}} + \Phi(1 - S_W)\cdot b}$$

$$V_p(S_W = 0.5) = \frac{1}{\frac{1}{V_{p(sat.)}} + \frac{1}{2}b\Phi}. \quad (9b)$$

Equalizing equations 9a and 9b

$$\frac{1}{V_{p(dry)}} - \frac{1}{2}a\Phi = \frac{1}{V_{p(sat.)}} + \frac{1}{2}b\Phi$$

$$\frac{1}{V_{p(dry)}} - \frac{1}{V_{p(sat.)}} = \frac{1}{2}(b + a)\Phi$$

and using the assumption $a = b$, the free parameter a can be determined by the following formula.

$$a = \frac{\frac{1}{V_{p(dry)}} - \frac{1}{V_{p(sat.)}}}{\Phi}. \quad (10)$$

Using the parameter *a*, the saturation dependent velocity can be calculated by the following two equations:

$$V_p(S_W) = \frac{1}{\frac{1}{V_{p(dry)}} - a\Phi S_W} \quad \text{for } S_W = 0.0.....0.5, \quad (11a)$$

$$V_p(S_W) = \frac{1}{\frac{1}{V_{p(sat.)}} + a\Phi(1 - S_W)} \quad \text{for } S_W = 0.5.....1.0. \quad (11b)$$

Compressional wave velocity values interpolated from dry samples and fully saturated samples at different saturation levels using equations 11a and 11b are listed in Table 5-4 of appendix 4 and shown in Fig. 5-7. It can be observed that the compressional wave velocities calculated at different saturation levels are close to the measured values.

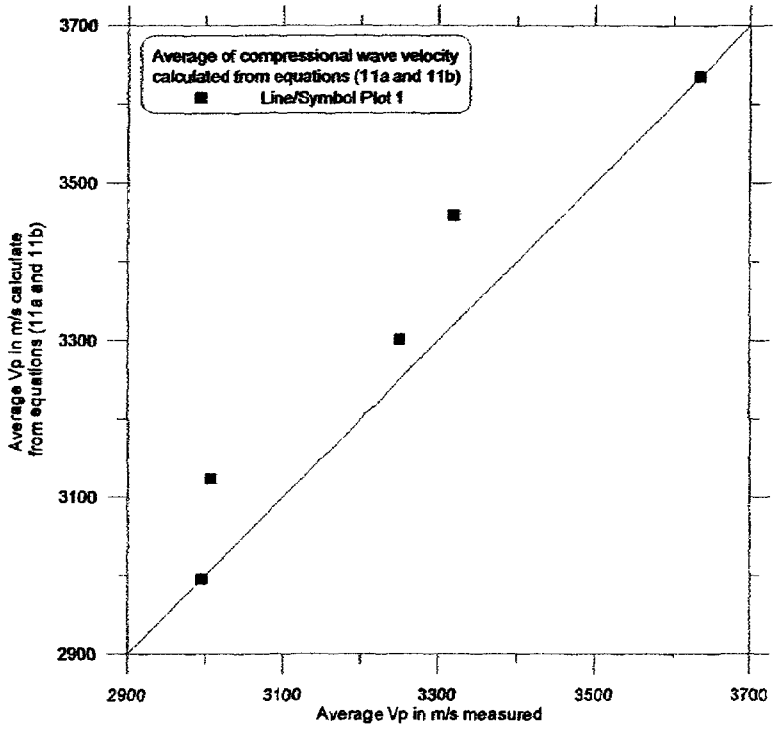

Fig. 5-7 Average of compressional wave velocity measured at different saturation levels versus average compressional wave velocity calculated from equations 11a and 11b.

5-5.2 Shear wave velocity and water saturation

Considering isotropic conditions, the shear wave velocity can be determined from the shear modulus μ and the density d of the material according to the equation **(Reynolds, 2005).**

$$V_S = \sqrt{\frac{\mu}{d}}. \qquad (12)$$

Using this equation, the shear modulus μ can be determined from the known s-wave velocity and known density in dry state of the sample:

$$\mu = V_{s(dry)}^2 \cdot d_{(dry)}$$

The saturation dependent bulk density can be determined using the mixing law

$$d(S_W) = d_{(grain)}(1-\Phi) + d_A(1-S_W).\Phi + d_W \Phi.S_W$$

That can be simplified assuming a vanishing air density ($d_A = 0$):

$$d(S_W) = d_{(grain)}(1-\Phi) + d_W \Phi . S_W$$

Under dry conditions with water saturation $S_W = 0$, we get

$$d(S_W = 0) = d_{(grain)}(1-\Phi) = d_{(dry)}. \qquad (13)$$

Under fully saturated condition with $S_W = 1$, we get

$$d(S_W = 1) = d_{(grain)}(1-\Phi) + d_W \Phi . \qquad (14)$$

Considering partial saturation with $0 < S_W < 1$, equation (12) is extended

$$V_S(S_W) = \sqrt{\frac{\mu}{d_{(grain)}(1-\Phi) + d_W \Phi S_W}} . \qquad (15)$$

For the numerical calculation, the following values are considered:

$d_{(grain)} \hat{=}$ average grain density of samples (≈ 2650 kg/m^3),

$\Phi \hat{=}$ average porosity of samples,

$d_W =$ water density (1000 kg/m^3).

Under dry conditions with water saturation ($S_W = 0$), $\mu(S_W = 0) = \mu_{(dry)}$, we get

$$d(S_W = 0) = d_{(grain)}(1-\Phi) = d_{(dry)} .$$

The resulting equation can be written in the form:

$$V_S(S_W) = \sqrt{\frac{V^2_{S(dry)} . d_{(grain)}(1-\Phi)}{d_{(grain)}(1-\Phi) + d_W \Phi S_W}} . \qquad (16)$$

Shear wave velocity values extrapolated from dry samples at different saturation levels according to equation 16 are listed in Table 5-6 of appendix 4 and shown in Fig. 5-8. It can be observed that the extrapolated shear wave velocities calculated at different saturation level show only a slight variation. The predicted velocity values are higher than the measured ones. The graph shows that the assumption that the shear modulus is independent of saturation is not valid.

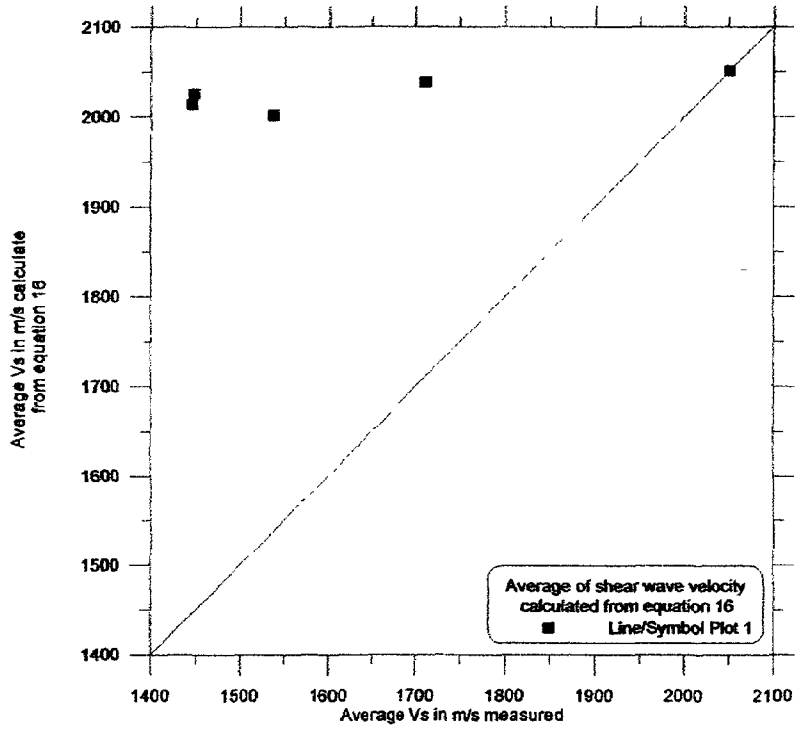

Fig. 5-8 Average of shear wave velocity measured at different saturation levels versus average shear wave velocity calculated from equation 16.

Under fully saturated condition with $(S_W = 1)$, $\mu(S_W = 1) = \mu_{(sat.)}$, we get

$$\mu_{(sat.)} = V^2_{S(sat.)}\left(d_{(grain)}(1-\Phi) + d_W\Phi\right).$$

The resulting equation can be written in the form:

$$V_S(S_W) = \sqrt{\frac{\mu(S_W)}{d_{(grain)}(1-\Phi) + d_W\Phi S_W}}. \qquad (17a)$$

An interpolation of the shear modulus between the dry and fully saturated state is proposed in the form:

$$\mu(S_W) = \mu_{(sat.)} + (\mu_{(dry)} - \mu_{(sat.)}).(1-S_W)^n. \qquad (17b)$$

The exponent $n = 5$ was determined by searching for the best fitting between measured and predicted velocities. Shear wave velocity values at different saturation levels have been interpolated from dry and fully saturated state using equations 17a and 17b. The data is listed in Table 5-7 of appendix 4 and shown in Fig. 5-9.

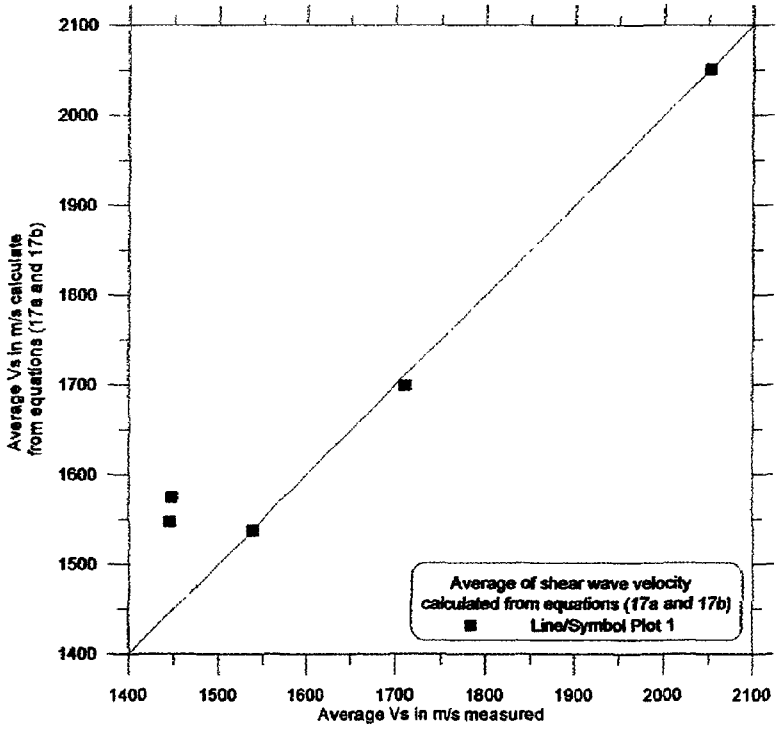

Fig. 5-9 Average of shear wave velocity measured at different saturation levels versus average shear wave velocity calculated from equations 17a and 17b.

5-5.3 Relation between Poisson's ratio and water saturation

Poisson's ratio is computed from p-wave velocity *Vp* and s-wave velocity *Vs* using the following relation:

$$\upsilon(S_W) = \frac{a(S_W) - 2}{2(a(S_W) - 1)}$$

with

$$a(S_W) = \left(\frac{V_P(S_W)}{V_S(S_W)} \right)^2 .$$

The calculated Poisson's ratio determined from compressional wave velocity data obtained from equations 11a and 11b and shear wave velocity data obtained from equations 17a and 17b is listed in Table 5-9 of appendix 4 and shown in Fig. 5-10. The calculated values are in good agreement with the values obtained from measured compressional and shear wave velocity. A good knowledge of the velocities at dry and fully saturated state provides the possibility for a reliable prediction of Poisson's ratio.

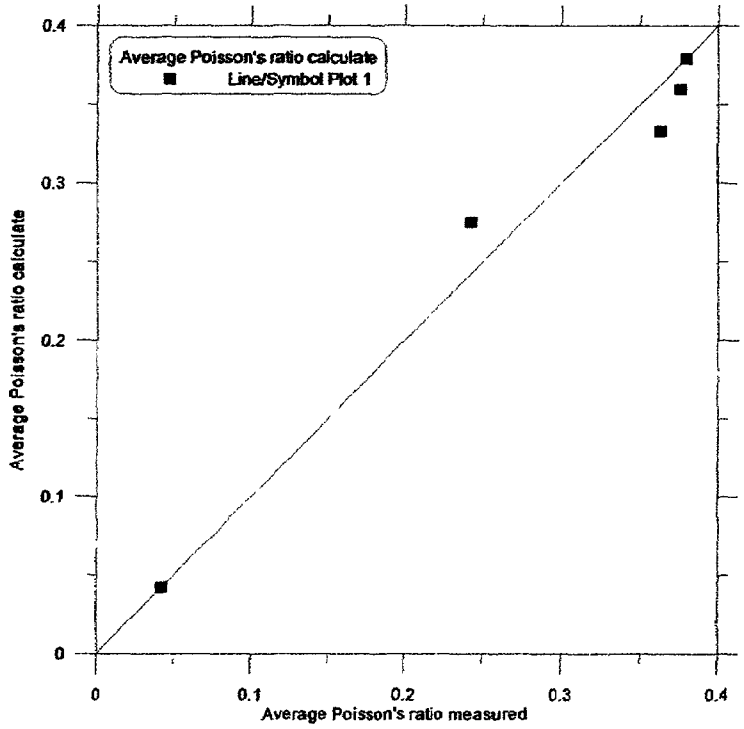

Fig. 5-10 Average of Poisson's ratio measured at different saturation levels versus average Poisson's ratio derived from interpolated values of p- and s-wave velocity.

5-5.4. Model of Wyllie and Raymer

The porosity can be derived from the knowledge of the interval velocity. The time average equation of **Wyllie et al. (1956 and 1958)** has been used to obtain porosity from acoustic velocity logs. This simple equation appears adequate for clean sandstone in the middle range of porosity ($10\% < \Phi < 25\%$). The equation for p-wave velocity Vp in water – saturated rock is:

$$\frac{1}{V_p} = \frac{\Phi}{V_f} + \frac{(1-\Phi)}{V_m} \qquad (18)$$

with:

V_p = compressional wave velocity,

V_m = velocity of the solid material,

V_f = velocity of the pore fluid,
(in dry condition: $S_W = 0$)

V_f = velocity in air.

The relationship between compressional wave velocity measured on dry samples versus compressional wave velocity calculated from Wyllie equation is shown in Fig. 5-11. Using $V_m \approx 4400 \ m/s$ and $V_f \approx 330 \ m/s$. In this graph, all data points are located below the diagonal line.

The relationship between compressional wave velocity measured on saturated samples versus compressional wave velocity calculated from Wyllie equation (only 26 samples used) is shown in Fig. 5-12. Using $V_m \approx 4400 \ m/s$ and $V_f \approx 1500 \ m/s$. It should be noted that the variation in the measured velocity is lower than in the predicted values for both dry and saturated samples. The data are listed in Tables 5-10, 11 of appendix 4.

Another empirical equation was proposed by **Raymer et al. (1980)** as an alternative to the time–average equation for interpretation of acoustic logs.

$$V_P = (1-\Phi)^2 . V_m + \Phi . V_f \qquad (19)$$

The relationship between compressional wave velocity measured on dry samples versus compressional wave velocity calculated from Raymer's equation is shown in Fig. 5-13. Taking $V_m \approx 6040 \ m/s$ results generally in higher predicted p-wave velocity. Using $V_m \approx 4400 \ m/s$ and $V_f \approx 330 \ m/s$ provides a better prediction.

The relationship between compressional wave velocity measured on saturated samples versus compressional wave velocity calculated from Raymer's equation (only 26 samples used) is shown in Fig. 5-14. Taking $V_m \approx 6040 \ m/s$ results generally in higher predicted p-wave velocity. Using $V_m \approx 4400 \ m/s$ and $V_f \approx 1500 \ m/s$ provides a better prediction. It should be noted that the variation in the measured velocity is larger than in the predicted values for both dry and saturated samples. The data are listed in Tables 5-10, 11 of appendix 4.

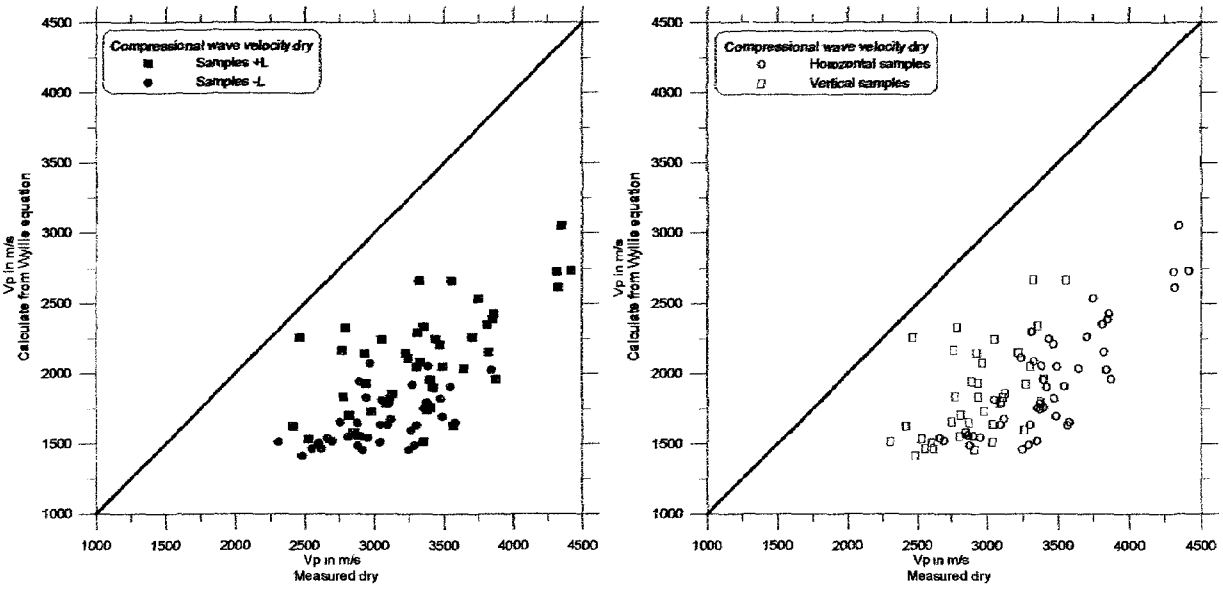

Fig. 5-11 Compressional wave velocity measured on dry samples versus compressional wave velocity calculated from Wyllie equation. 96 data points are used.

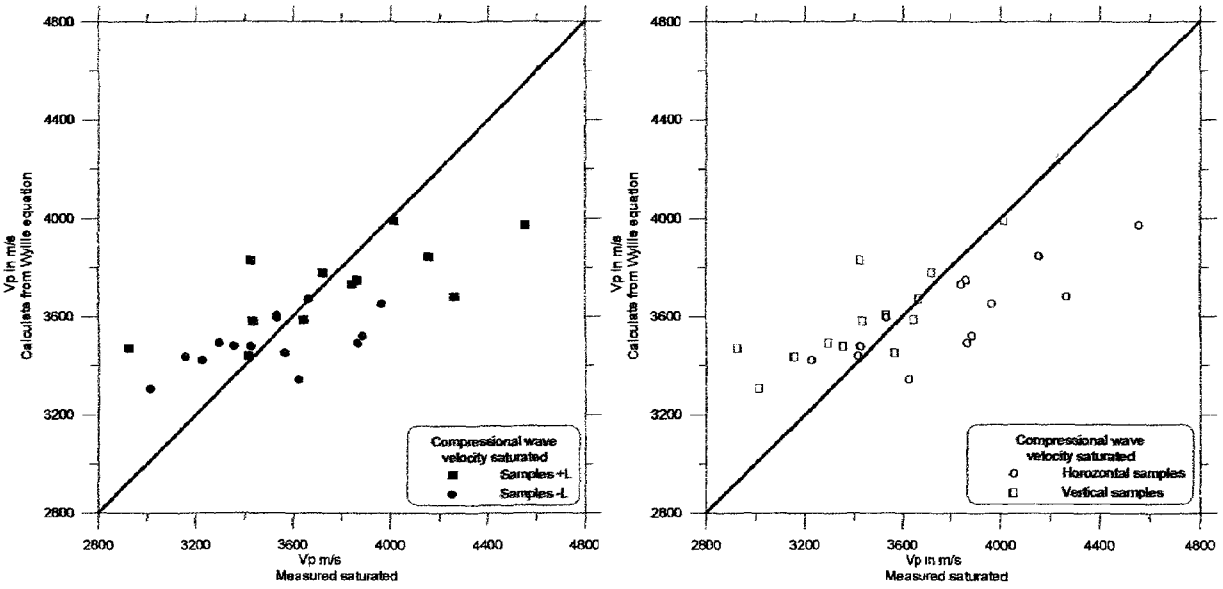

Fig. 5-12 Compressional wave velocity measured on saturated samples versus compressional wave velocity calculated from Wyllie equation. 26 data points are used.

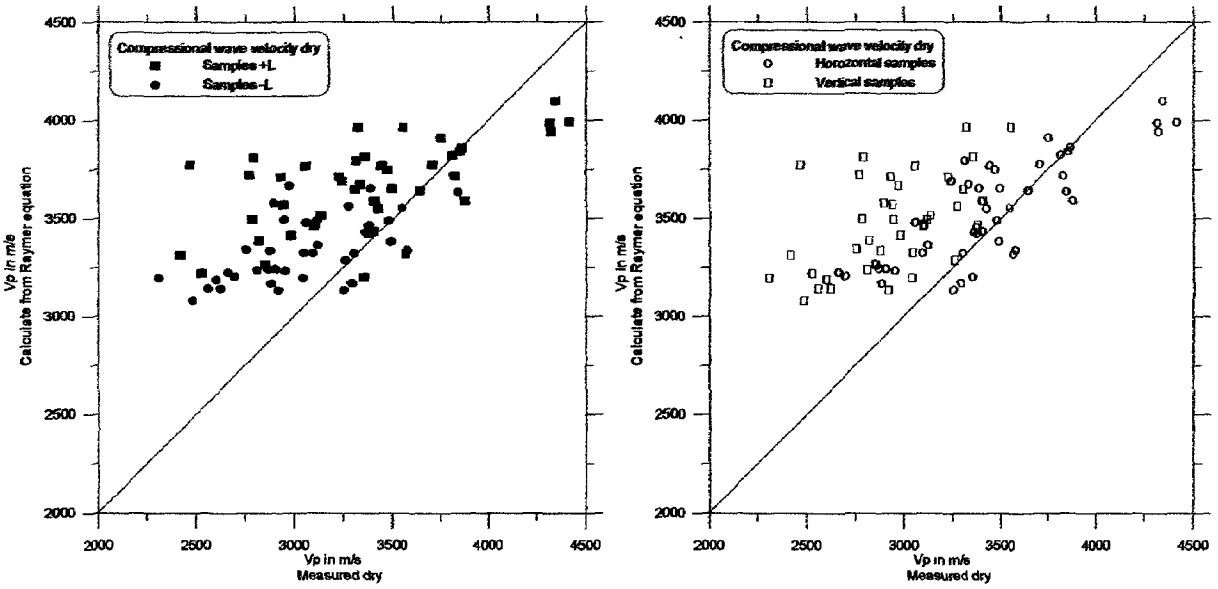

Fig. 5-13 Compressional wave velocity measured on dry samples versus compressional wave velocity calculated from Raymer's equation. 96 data points are used.

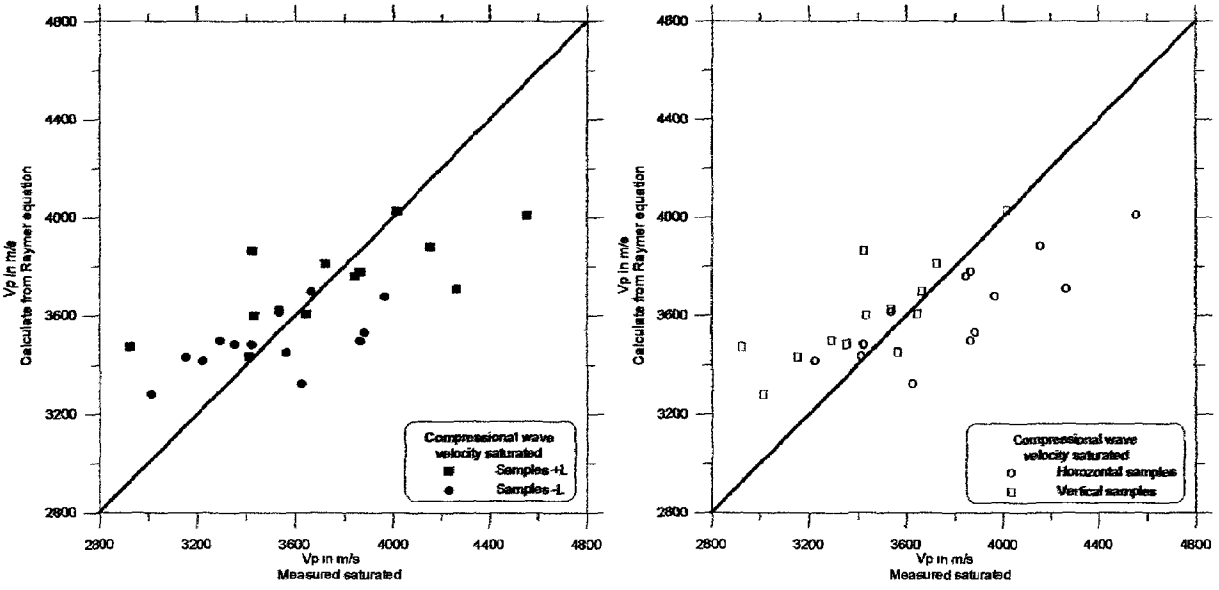

Fig. 5-14 Compressional wave velocity measured on saturated samples versus compressional wave velocity calculated from Raymer's equation. 26 data points are used.